Formation of $Zr_{70}Ni_{23}Ti_7$ glassy alloy and phase transformation upon annealing

Limin Wang[a] and Chunfei Li
Inoue Superliquid Glass Project, ERATO, JST, Sendai 982-0807, Japan
Liqun Ma and Akihisa Inoue
Institute for Materials Research, Tohoku University, Sendai 980-8577, Japan

(Received 13 June 2001; accepted 9 January 2002)

$Zr_{70}Ni_{23}Ti_7$ alloy contains a single amorphous phase when it is melt-spun at a wheel surface velocity over 20 m/s. The crystallization of these amorphous ribbons takes place through two exothermic reactions and shows a significant supercooled liquid region of about 30 K, indicating that the $Zr_{70}Ni_{23}Ti_7$ alloy has a good glass-forming ability. The crystallization products of the first exothermic reaction for the ribbon prepared at a wheel surface velocity of 40 m/s are mainly an icosahedral quasicrystalline phase (I-phase) and some Zr_2Ni phases. Further heating to a higher temperature will lead to the transformation of the metastable I-phase to Zr_2Ni. Some icosahedral atomic clusters with a structure similar to those in face-centered-cubic Zr_2Ni may exist in the alloy after rapid quenching, and most of them may act as nuclei of I-phase. The formation of I-phase in this alloy without any noble metals may be due to the proper atomic ratios in the system.

I. INTRODUCTION

The precipitation of icosahedral quasicrystalline phases (I-phase) from Zr-based amorphous alloys was reported initially by Köster *et al.*[1] Recently, much attention has been paid to amorphous Zr–Al–TM–M (TM = Co, Ni, Cu; M = Ag, Pd, Au, or Pt) systems[2–4] and Zr–TM–M systems[5–7] for the formation of I-phases from amorphous phases by crystallization. The typical alloy compositions for the Zr–Al–TM–M system are $Zr_{65}Al_{7.5}Ni_{10}Cu_{12.5}M_5$. In these alloys, noble metals (Pd, Pt, Au, and Ag) are added to the well-known good metallic glass forming $Zr_{65}Al_{7.5}Ni_{10}Cu_{17.5}$[8] to acquire and stabilize I-phases. For the Zr–TM–M system, the noble metals also play an important role in the formation of I-phases. For example, no icosahedral phase was observed in the $Zr_{70}(Ni,Cu)_{30}$ amorphous alloys; addition of Pd was found to be effective in promoting the formation of an I-phase.[7] It has also been noticed that most of the above amorphous alloys exhibit a significant supercooled liquid region, $\Delta T_x = T_x - T_g$, where T_x and T_g are the crystallization and glass transition temperature, respectively. The existence of a supercooled region usually corresponds to a good glass-forming ability of an amorphous alloy. There are few resports on formation of an I-phase from Zr-based amorphous alloys with high Zr content and without any noble metals.

II. EXPERIMENTAL

The alloy ingots of $Zr_{70}Ni_{23}Ti_7$ were prepared by arc melting a mixture of pure metals in an argon atmosphere. From these alloy ingots, ribbons were prepared by a single roller melt-spinning method at different wheel surface velocities in an argon atmosphere. The thickness of the ribbons was about 20–45 μm; the width of the cross-section of the ribbons was about 1.0–1.3 mm. The structure was examined by x-ray diffraction (XRD) and the thermal stability was evaluated by differential scanning calorimetry (DSC) at a heating rate of 0.67 K/s. The microstructure was examined by transmission electron microscope (TEM) JEM-3000F operated at 300 kV. The diameter of the electron beam was focused to 1.0 nm during nanobeam electron diffraction.

III. RESULTS AND DISCUSSIONS

A. Phases by melt-spinning and annealing

Figure 1 shows the XRD patterns of the melt-spun $Zr_{70}Ni_{23}Ti_7$ ribbons prepared at different wheel surface velocities. The two halo-rings indicate that the melt-spun

[a]Address all correspondence to this author.
e-mail: wang@sendai.jst.go.jp

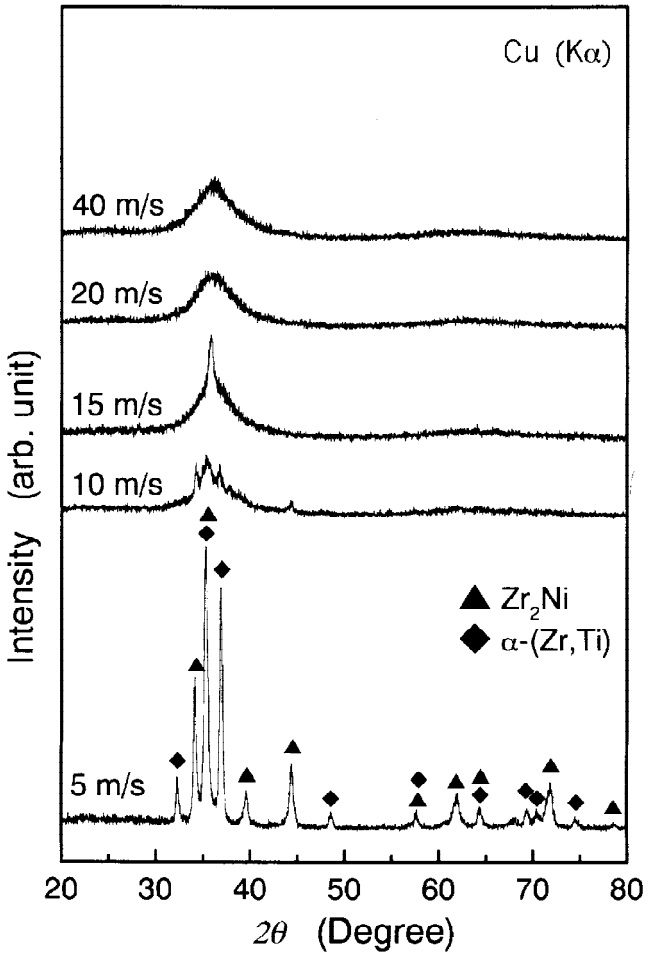

FIG. 1. XRD patterns of the melt-spun $Zr_{70}Ni_{23}Ti_7$ ribbons prepared at different wheel surface velocities.

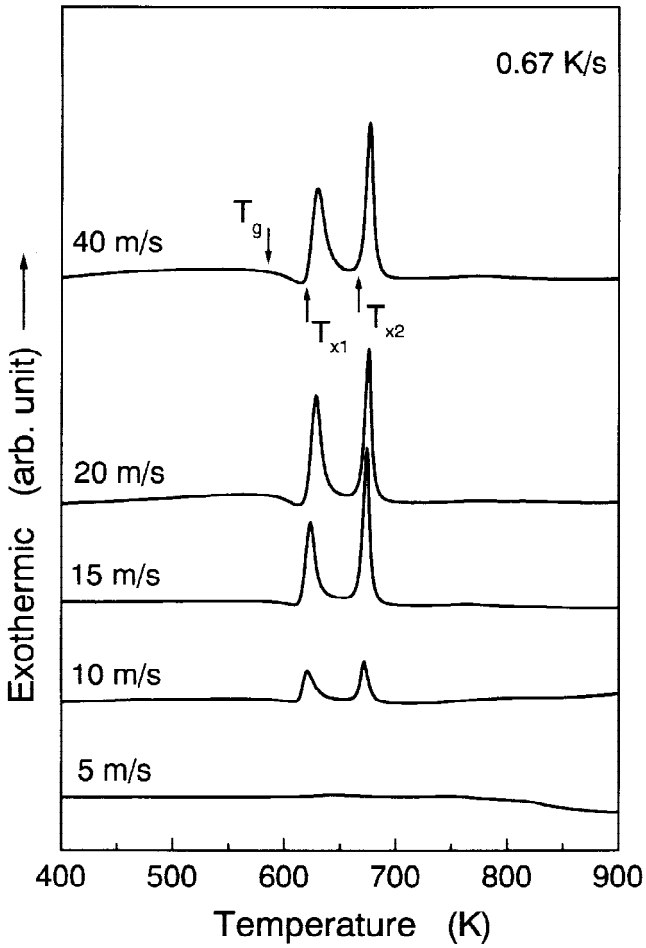

FIG. 2. DSC curves of the melt-spun $Zr_{70}Ni_{23}Ti_7$ ribbons.

ribbons were in a glassy state when the wheel surface velocity was over 20 m/s. It is also clear that the ribbons consisted of crystalline and glassy phases when the velocity was in the range of 10–15 m/s. No amorphous phases were seen when the wheel surface velocity was 5 m/s. In this case, the crystalline phases were identified as Zr_2Ni and α–(Zr, Ti).

Figure 2 shows the DSC curves of the melt-spun ribbons. The crystallization of all the ribbons that contain amorphous phases took place through two exothermic reactions. When the wheel surface velocity was over 20 m/s—i.e., the melt-spun ribbons were in an amorphous state—supercooled liquid regions beginning with the marked glass transition temperature T_g appeared. The width of the supercooled liquid regions, $\Delta T_x = T_x - T_g$, was about 30 K, indicating that this $Zr_{70}Ni_{23}Ti_7$ amorphous alloy exhibits good glass-forming ability.

Figure 3 shows the XRD patterns of $Zr_{70}Ni_{23}Ti_7$ ribbon samples prepared in the amorphous state by melt spinning at a wheel surface velocity of 40 m/s and subsequently annealed in the DSC cell with a heating rate of 0.67 K/s to 595, 605, 620, 640, 655, and 1000 K. The diffraction peaks of the ribbon samples heated to the range of 605 to 640 K, which correspond to the first exothermic reaction, were identified as mainly corresponding to the I-phase and smaller fraction of some Zr_2Ni phases. Further annealing to 655 K led to the transformation of the I-phase to Zr_2Ni, indicating that the I-phase was in a metastable state. The stable crystallization products were Zr_2Ni and α–(Zr, Ti) when the ribbon was heated to 1000 K.

Figure 4(a) shows a bright-field TEM image of the $Zr_{70}Ni_{23}Ti_7$ ribbon annealed to 640 K. The size of the precipitated particles was less than 50 nm. Figures 4(b), 4(c), and 4(d) show the selected-area electron diffraction pattern, the nanobeam electron diffraction pattern corresponding to fivefold symmetries of the I-phase, and the electron diffraction pattern of the Zr_2Ni phase, respectively. From these diffraction patterns, it was firmly established that the initial precipitation phases were an I-phase and a Zr_2Ni phase.

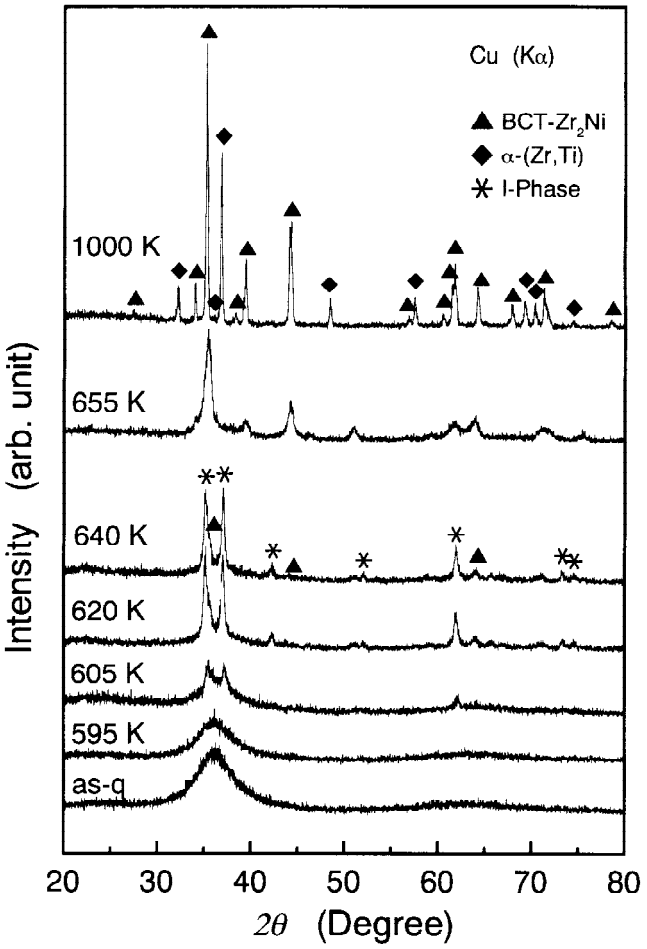

FIG. 3. XRD patterns of the annealed samples of the amorphous phase $Zr_{70}Ni_{23}Ti_7$ ribbon prepared at a wheel surface velocity of 40 m/s.

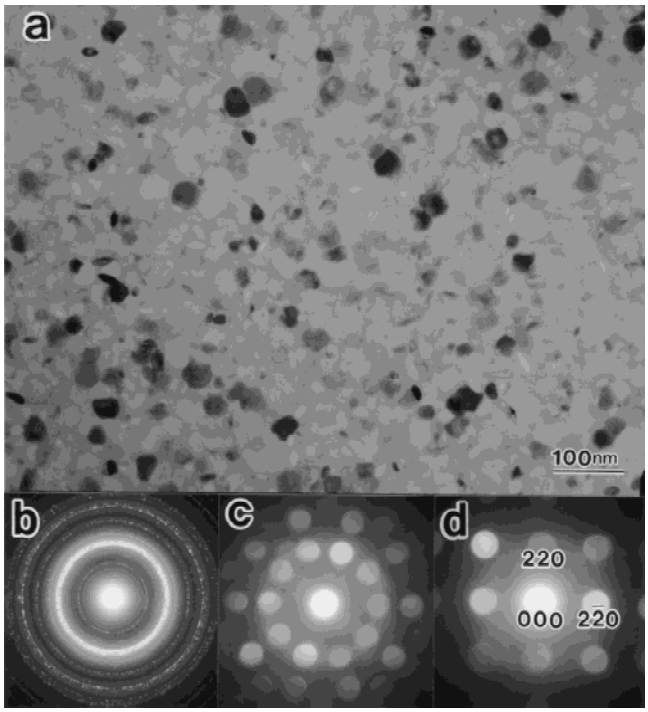

FIG. 4. (a) Bright-field TEM image, (b) selected-area electron diffraction pattern, (c) the nanobeam electron diffraction pattern corresponding to fiveold symmetries of the I-phase, and (d) electron diffraction pattern for [00$\bar{1}$] of the Zr_2Ni phase of the amorphous $Zr_{70}Ni_{23}Ti_7$ alloy annealed to 640 K.

B. Formation of I-phase

Two significant metastable phases were found in the initial crystallization process of Zr-based amorphous alloys, i.e., the face-centered cubic (fcc) Zr_2Ni (cubic, $Fd\bar{3}m$, $a = 1.227$ nm)[9] and the I-phase.[2,4,10] The structures of fcc-Zr_2Ni and I-phase are characterized by the possession of icosahedral atomic clusters in their local atomic configurations.[13,14] Therefore, it has been speculated that icosahedral atomic clusters exist in the melt, and some of them are retained during the rapid quenching. It is suggested from the above-described results of the $Zr_{70}Ni_{23}Ti_7$ alloy that such icosahedral atomic clusters should exist in this alloy after rapid quenching. These clusters may have a structure similar to those in fcc-Zr_2Ni. Some of them act as nuclei to the I-phase during the first exothermic reaction. This speculation is also supported by the consideration of atomic radii and heats of mixing. The negative heats of mixing are 0, −35, and −49 kJ/mol for Zr–Ti, Ti–Ni, and Ni–Zr atomic pairs, respectively. The strong binding between Ti–Ni and Ni–Zr atomic pairs implies that Ni atoms tend to be surrounded by as many as possible Zr/Ti atoms. Formation of an icosahedral atomic cluster with the center site occupied by Ni atom satisfied the above-mentioned requirement. Such clusters may serve as the nuclei for the precipitation of I-phase. The radius of atom occupying the center site of a regular icosahedron should be approximately 5% smaller than those occupying the vertices. Considering the atomic radii of Ni (0.1285 nm), Ti (0.147 nm), and Zr (0.162 nm), it is recognized that Ti atom is more suitable to vertice sites. In other words, the partial substitution of Zr by Ti in Zr–Ni system makes the formation of icosahedral atomic cluster easy and the formed cluster more stable. This, in turn, promotes the formation of the I-phase in the initial crystallization process.

It has been reported that the valence electron concentration per atom (e/a) is an important factor affecting the formation of an I-phase. However, a discussion of the I-phase stability in term of e/a value for the Zr-based system is not straightforward in the present state. This is illustrated as follows by considering the Zr–Ni,[9] Zr–Ni–Ti, Zr–Cu–Pd,[15] and Zr–Ni–Pd[16] systems. The valence electron contributions proposed for Zr, Ti, Ni, and Cu are 1.1, −1, −1, and 1, respectively. First, we compare Zr–Ni and Zr–Ni–Ti systems. These two systems have different e/a values and show different

behaviors in the formation of an I-phase—i.e., a metastable I-phase was found in the initial crystallization process of Zr–Ni–Ti while no I-phase was reported in that of Zr–Ni. The e/a values are different for the Zr–Cu–Pd and Zr–Ni–Pd systems, too. However, I-phase was reported in both systems. It seems that more work, especially theoretical prediction for the valence electron contribution, are required to perform a detailed discussion of the Zr-based I-phase stability in terms of e/a value.

REFERENCES

1. U. Köster, J. Meinhardt, S. Roos, and H. Libertz, Appl. Phys. Lett. **69,** 179 (1996).
2. M.W. Chen, T. Zhang, A. Inoue, A. Sakai, and A. Sakurai, Appl. Phys. Lett. **75,** 1697 (1999).
3. A. Inoue, T. Zhang, J. Saida, M. Matsusita, M.W. Chen, and T. Sakurai, Mater. Trans. JIM **40,** 1137 (1999).
4. A. Inoue, T. Zhang, J. Saida, M. Matsusita, M.W. Chen, and T. Sakurai, Mater. Trans. JIM **40,** 1181 (1999).
5. M. Matsushita, J. Saida, C. Li, and A. Inoue, J. Mater. Res. **15,** 1280 (2000).
6. J. Saida, M. Matsushita, C. Li, and A. Inoue, Appl. Phys. Lett. **76,** 3558 (2000).
7. T. Zhang, A. Inoue, M. Matsushita, and J. Saida, J. Mater. Res. **16,** 20 (2001).
8. A. Inoue, T. Zhang, N. Nishiyama, K. Ohba, and T. Masumoto, Mater. Trans. JIM **34,** 1234 (1993).
9. Z. Altounian, E. Batalla, J.O. Strom-Olsen, and J.L. Walter, J. Appl. Phys. **61,** 149 (1987).
10. Q.B. Yang, Philos. Mag. Lett. **57,** 171 (1988).
11. J. Saida, M. Matsushita, C. Li, and A. Inoue, Philos. Mag. Lett. **80,** 737 (2000).
12. M. Matsushita, J. Saida, and A. Inoue, Philos. Mag. Lett. **80,** 79 (2000).
13. J. Eckert, N. Mattern, M. Zinkevitch, and M. Seidel, Mater. Trans. JIM **39,** 623 (1998).
14. A. Inoue, T. Zhang, M.W. Chen, T. Sakurai, J. Saida, and M. Matsushita, J. Mater. Res. **15,** 2195 (2000).
15. M. Matsushita, J. Saida, C. Li, and A. Inoue, J. Mater. Res. **15,** 1280 (2000).
16. J. Saida, M. Matsushita, C. Li, and A. Inoue, Appl. Phys. Lett. **76,** 3558 (2000).